19951224 20

N95- 28841

DESIGN AND EVALUATION OF A FOAM-FILLED HAT-STIFFENED PANEL CONCEPT FOR AIRCRAFT PRIMARY STRUCTURAL APPLICATIONS

Damodar R. Ambur
NASA Langley Research Center
Hampton, VA 23665-5225

5/8-05

INTRODUCTION

Geodesically stiffened structures are very efficient in carrying combined bending, torsion, and pressure loading that is typical of primary aircraft structures. They are also very damage tolerant since there are multiple load paths available to redistribute loads compared to prismatically stiffened structures (Refs. 1,2). Geodesically stiffened structures utilize continuous filament composite materials which make them amenable to automated manufacturing processes to reduce cost. The current practice for geodesically stiffened structures is to use a solid blade construction for the stiffener. This stiffener configuration is not an efficient concept and there is a need to identify other stiffener configurations that are more efficient but utilize the same manufacturing process as the solid blade.

This paper describes a foam-filled stiffener cross section that is more efficient than a solid-blade stiffener in the load range corresponding to primary aircraft structures. A prismatic hat-stiffener panel design is then selected for structural evaluation in uni-axial compression with and without impact damage. Experimental results for both single stiffener specimens and multi-stiffener panel specimens are presented. Finite element analysis results are presented that predict the buckling and postbuckling response of the test specimens. Analytical results for both the element and panel specimens are compared with experimental results.

FOAM-FILLED STIFFENER CONCEPT

In order to make the solid-blade stiffener shown in Figure 1 more efficient, it is necessary to position the 0° material away from the skin to increase the bending stiffness. When such a stiffener concept is applied to a geodesically stiffened structural configuration, the tooling design becomes extremely complicated if the tooling must be removed after curing. It is cost effective to leave the tooling in the hat stiffener if the material for the tool is light in weight and has the necessary processing characteristics for curing and adequate mechanical properties to support the stiffener and skin elements when loaded. In a typical manufacturing process, the overwrap material is first placed in a female tool and unidirectional material is tow placed to form a predominantly 0° material stiffener cap. A pre-machined foam insert is then placed in the tool to complete the stiffener. Skin material of the required thickness is then tow placed to complete the assembly which is then cured to produce the geodesically stiffened structure. As a first step toward evaluating this stiffener concept for geodesically stiffened structures, a prismatic stiffener panel study was undertaken which is the subject of this paper.

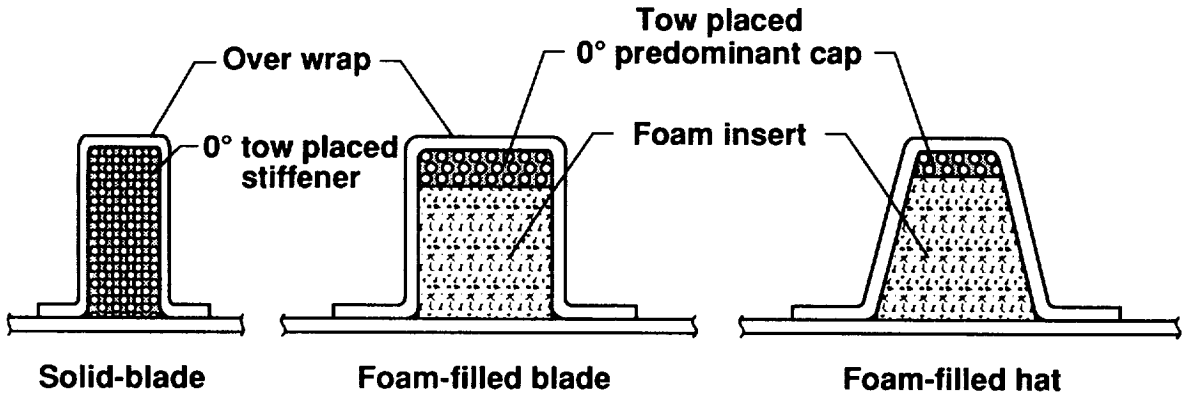

Figure 1. Foam-filled stiffener concepts.

STRUCTURAL EFFICIENCY OF FOAM-FILLED-STIFFENER PANEL CONCEPTS

A design study was performed to compare the structural efficiency of the foam-filled structural concepts with the simpler, efficient, and more widely used hat-stiffener concept. The results presented in Figure 2 correspond to a 30-inch-long and 24-inch-wide panel with four stiffeners across the width. The unidirectional tape material used in this study is the Hercules Inc. AS4/3502 graphite-epoxy system with Rohacell WF-71 foam as the core material. This four-stiffener configuration is structurally the most efficient for load cases above 6,000 lb/in. and has also been adapted for lower load cases in this study. A constrained optimization for minimum weight was performed using the Panel Analysis and Sizing COde (Ref. 3) and the results for a range of axial loads from 3,000 to 20,000 lb/in. are presented herein. Results for solid-blade stiffened panel are also included in this figure for reference.

The results show that the foam-filled hat-stiffened panel is lighter than the conventional hat-stiffened panel by about 6.5 percent at 6,000 lb/in. and by about 10 percent at 20,000 lb/in. The foam-filled blade-stiffened panel appears to perform better than the hat-stiffened panel above 16,000 lb/in. The foam-filled hat-stiffener panel is lighter by about 20 percent when compared to the solid-blade concept. Hence, If the foam-filled hat-stiffened concept is used in stiffened structures, a substantial weight savings is possible over the entire load range considered. A foam-filled hat-stiffener panel design for 3,000 lb/in., which corresponds to a fuselage structure, has been chosen for further evaluation.

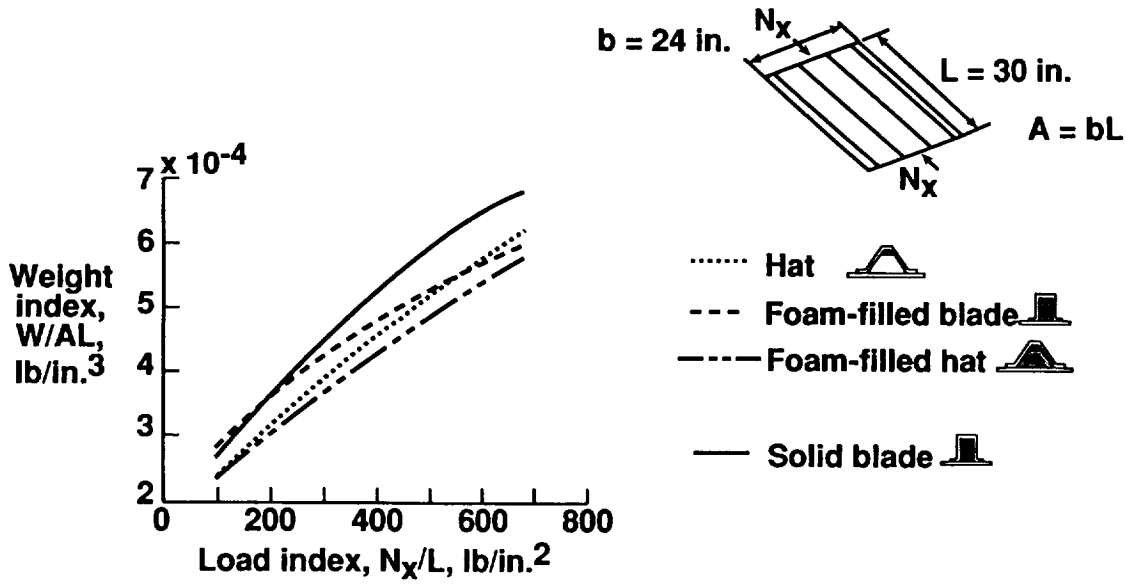

Figure 2. Structural efficiency of foam-filled stiffener panel concepts.

FOAM-FILLED HAT-STIFFENED PANEL SPECIMEN

A photograph of the foam-filled hat-stiffened panel is shown in Figure 3. The ends of the panel were potted, and machined flat and parallel to introduce load. The sides of the panel were simply-supported using knife edges. The ply layup for the skin, stiffener cap, and stiffener web are provided in this figure. The plies in all structural elements are oriented in at least three directions for laminate stability.

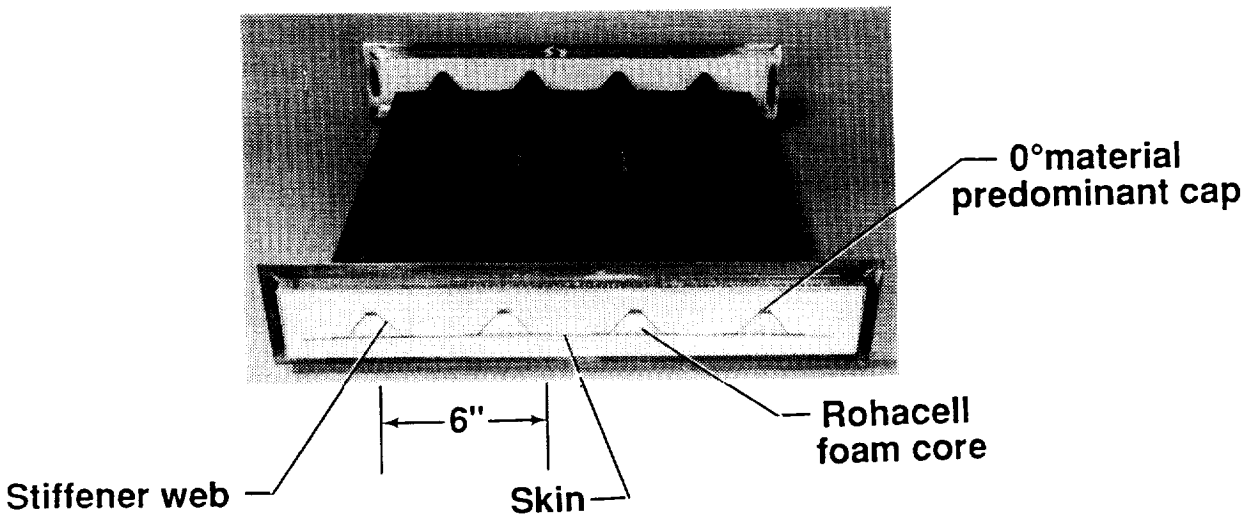

- **Ply layup**
  - **Skin:** $(\pm 45/\mp 45/\pm 45/\mp 45/0)_s$
  - **Stiffener cap:** $(\pm 45/0_5/-45/0_5/45/0_5/\overline{90})_s$
  - **Stiffener web:** $(\pm 45/\mp 45/\overline{90})_s$

Figure 3. Laminate details of foam-filled hat-stiffened panel.

FAILURE MODE OF ELEMENT SPECIMEN WITHOUT DAMAGE

The element specimen is a single stiffener structure which was tested as a wide column. For this test, strain gages were placed at the mid-length of the specimen on the stiffener cap, skin, and skin-stiffener flange locations. Displacement transducers were used to monitor specimen end-shortening and out-of-plane displacements and shadow moire interferometry was used to obtain a field view of the out-of-plane displacement contours.

As the specimen was loaded, the skin buckled first at about 33,500 lb and further loading of the element specimen resulted in failure at 36,080 lb. The out-of-plane displacement contour of the specimen is shown on the left of Figure 4. At the instance of failure, the skin had seven half-waves along the length of the specimen. The failure appeared to initiate along the nodal line slightly below the mid-length of the specimen due to high interlaminar stresses and propagated across the width of the specimen as shown on the right of the figure. The failure is characterized by a clean break of the foam-filled stiffener.

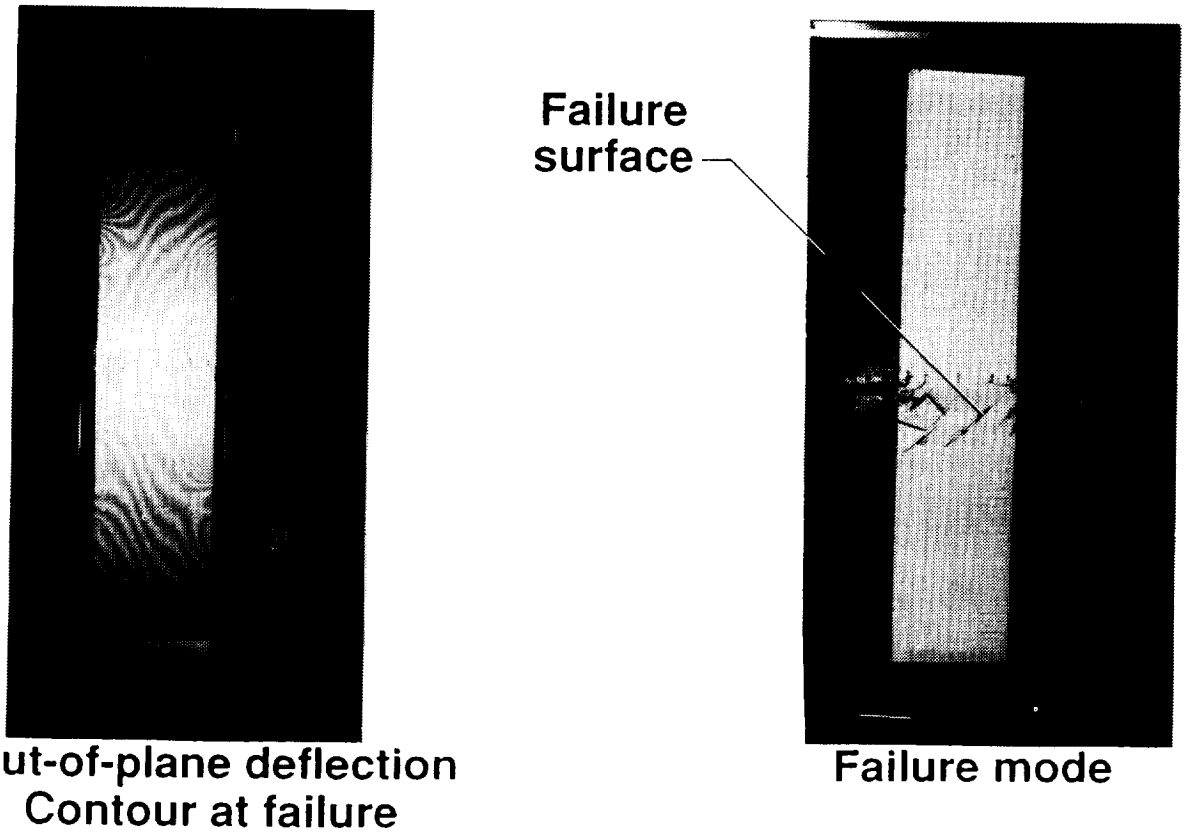

Figure 4. Failure mode of undamaged element specimen.

FAILURE MODE OF ELEMENT SPECIMEN WITH DAMAGE AT STIFFENER CAP

The element specimen was impact damaged by dropping a weight on the stiffener cap. This test was intended to simulate impact to the interior of the structure by dropped tools during manufacturing and servicing. Several impact tests were performed on additional specimens at increasing energy levels to determine the magnitude of the energy that caused barely visible damage to occur. This threshold level was determined to be 15 ft-lb for the stiffener cap. The rationale is that if the damage is visible the structure will be repaired or replaced before flying the aircraft.

The location of impact is at mid-length of the specimen as shown in Figure 5. An impact energy level of 20 ft-lb was chosen as an upper bound for impact. As the specimen was loaded with the damage resulting from this impact, the specimen skin buckled at approximately 33,500 lb and the final failure of the specimen occured at 35,552 lb. The failure mode was very similar to the element specimen without impact damage. This result suggests that the imposed damage scenario of 20 ft-lb on the stiffener cap does not result in any reduction in residual strength.

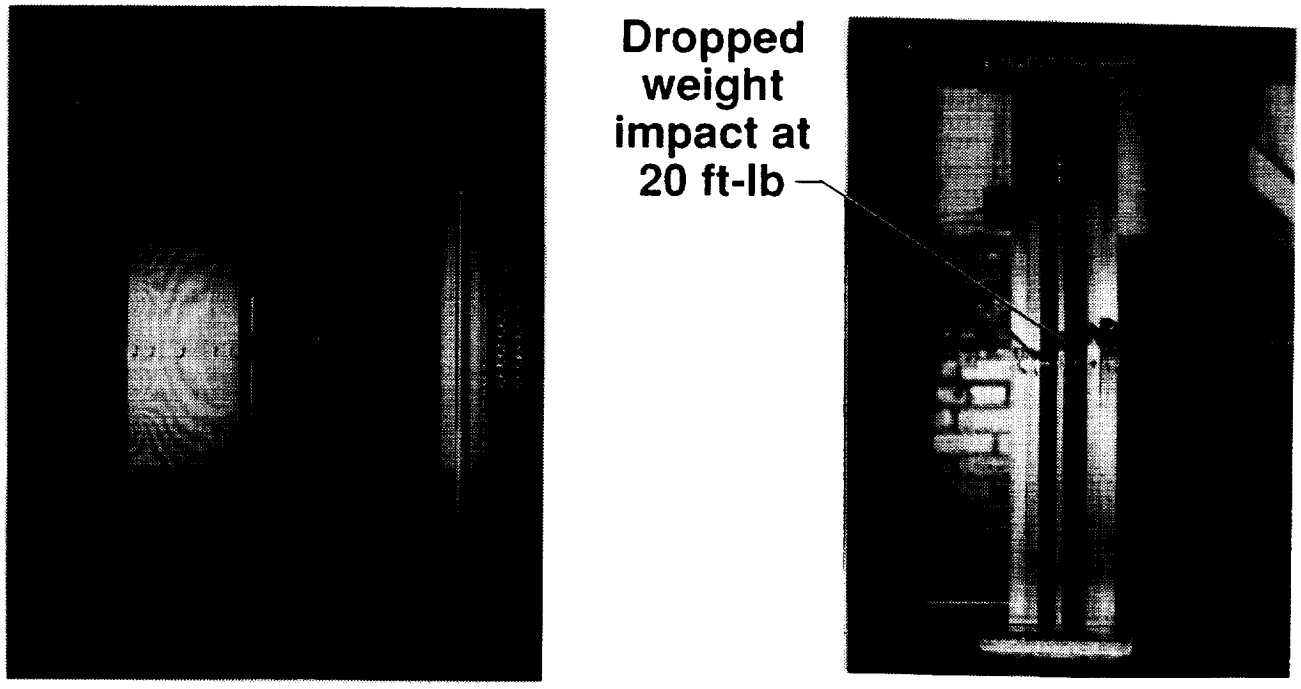

Figure 5. Failure mode of element specimen subjected to dropped-weight impact.

FAILURE MODE OF ELEMENT SPECIMEN WITH DAMAGE AT SKIN-STIFFENER FLANGE INTERFACE LOCATION

An element specimen was subjected to damage on the skin side of the specimen by an airgun-propelled impacter. This damage was intended to simulate impact to the exterior of the structure due to runway debris and hailstones. A barely visible damage criterion was also used in this case. Several impact tests were performed on additional specimens at increasing levels of airgun impact velocity to determine the threshold velocities for both skin and skin-stiffener flange interface locations. The velocities corresponding to barely visible damage are 125 ft/sec and 150 ft/sec for the skin and skin-stiffener flange interface locations, respectively. The actual impact velocities selected were 150 ft/sec for the skin and 175 ft/sec for the skin-stiffener interface locations. Since the skin-stiffener interface location is more critical, the element specimen was impacted at the skin-stiffener interface location. The location of impact is shown in Figure 6.

Failure initiated from the impact damaged skin-stiffener flange interface location and propagated across the width of the specimen before skin could buckle and propagated across the width of the specimen in a catastrophic manner. The specimen failed at 31,304 lb which is 15 percent lower than the undamaged element specimen failure load. The failure mode is shown on the right of the figure.

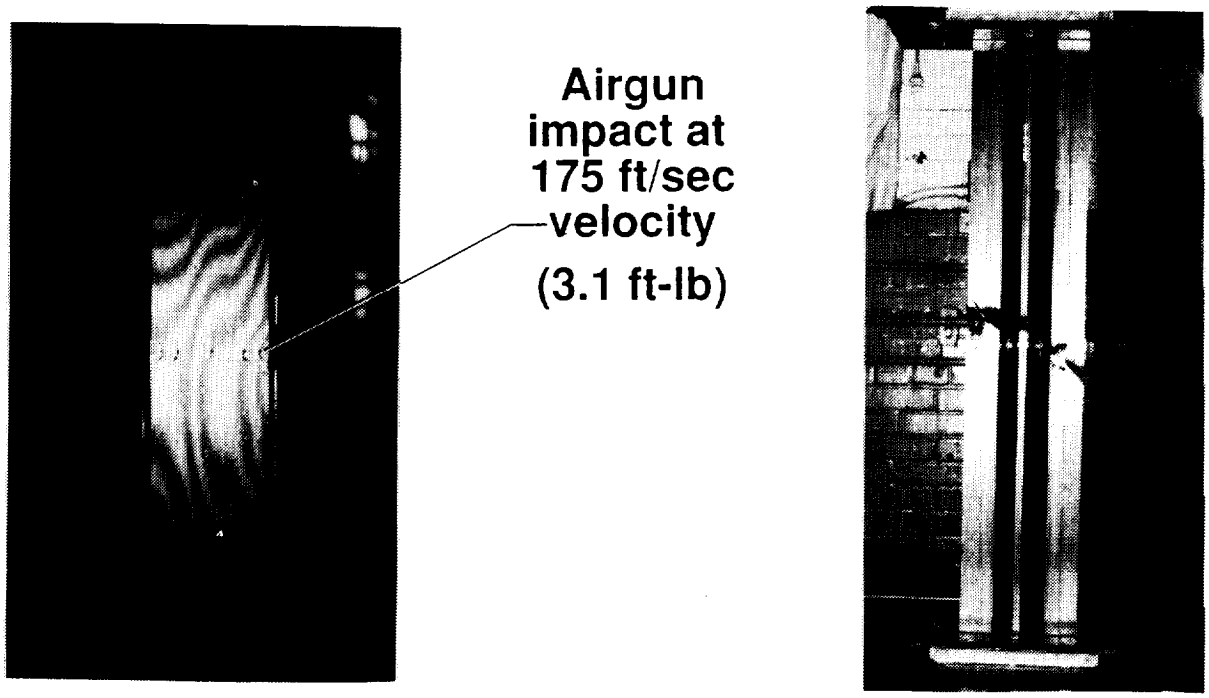

Figure 6. Failure mode of element specimen subjected to airgun impact.

END-SHORTENING RESPONSE FOR ELEMENT TEST SPECIMENS

The end-shortening results for the element test specimens are summarized in Figure 7. In this figure, end-shortening results are normalized by the overall length of the specimen and then plotted against the total applied load normalized by the axial stiffness of the specimen. Thus, the numbers along the axes represent global axial strains. The open circles, squares, and triangles represent data for specimens without damage, with airgun impact damage, and with dropped-weight impact damage, respectively. The solid symbols represent the corresponding failure events. All specimens exhibit nonlinear behavior beyond approximately 33,000 lb, which is the load at which skin buckling occurred. The specimens without damage and dropped-weight impact damage failed at an axial strain of 7,500μ in./in. while the specimen with airgun impact damage at the skin-stiffener flange interface location failed at 6,000μ in./in.

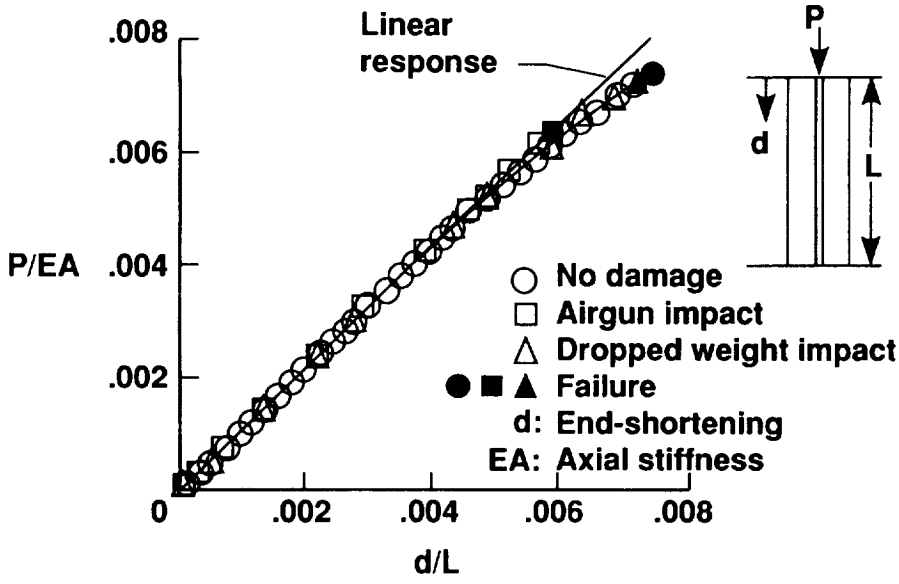

Figure 7. Summary of load versus end-shortening results for element test specimens.

STRAIN RESULTS FOR ELEMENT TEST SPECIMEN WITHOUT DAMAGE

The strain results for the undamaged element specimen are plotted in Figure 8. The strain gages are mounted across the specimen at mid-length. All gages except gage 2 indicate a similar global bending trend which is nonlinear beyond approximately 15,000 lb. The initial response of gage 2 suggests local bending of the skin element under the stiffener and strain reversal at about 33,000 lb indicates local buckling of skin. The maximum value of the local strains at failure is approximately 7,500μ in./in.

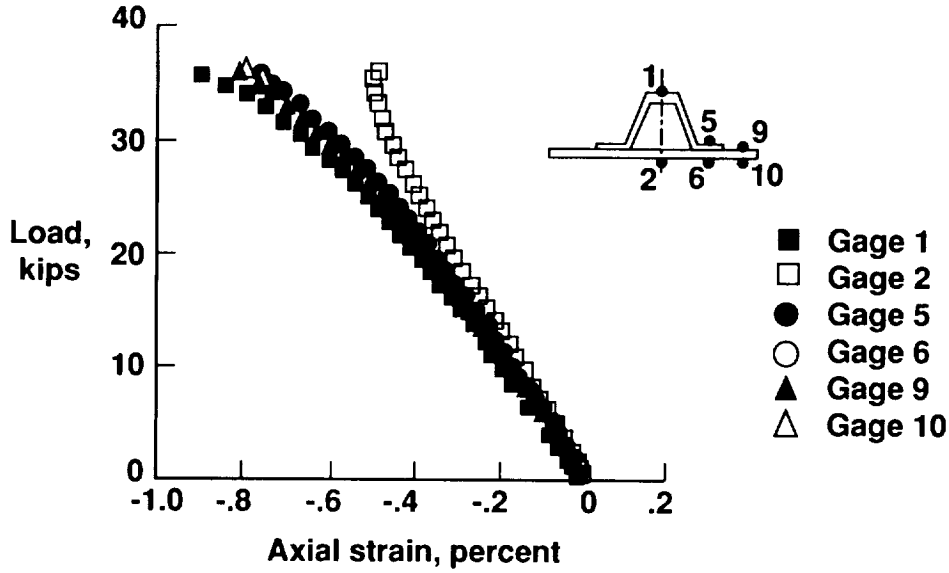

Figure 8. Axail strain results for undamaged element test specimen.

FAILURE MODE OF PANEL SPECIMEN WITHOUT DAMAGE

The panel test specimens were instrumented with strain gages, displacement transducers, and shadow moire interferometry to monitor local strains, out-of-plane and end-shortening displacements. As this undamaged panel specimen was loaded, it exhibited observable out-of-plane displacement at about 50,000 lb in the form of two lobes that were observed at the left and right of the specimen as shown in Figure 9. As the loading was increased, the skin in the central bay of the specimen buckled at approximately 125,000 lb with further loading resulting in failure of the specimen at 133,828 lb. The out-of-plane displacement contour at failure is shown on the left of the figure. The failure appears to have originated along the skin buckle nodal line below the mid-length of the specimen. The failure propagated catastrophically following the nodal line direction to the boundaries. The failure surface of the specimen is shown on the right of the figure.

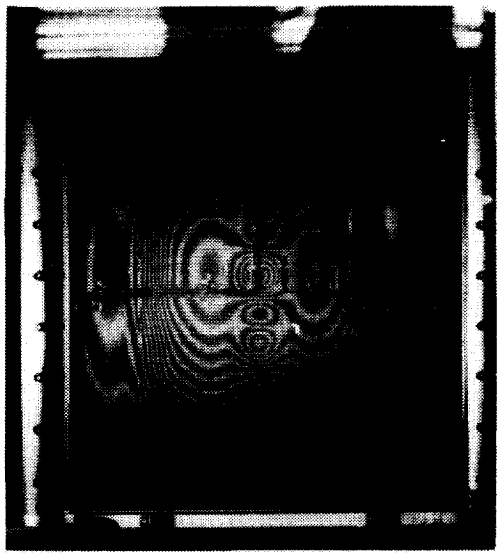

Out-of-plane displacement Contour at failure

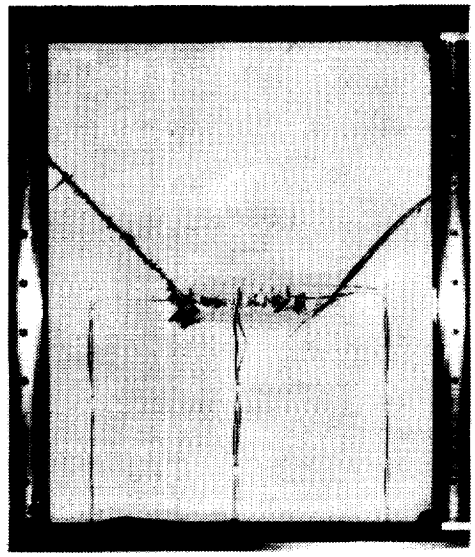

Failure mode Skin side

Figure 9. Failure mode of undamaged panel specimen.

FAILURE MODE OF PANEL SPECIMEN WITH AIRGUN IMPACT DAMAGE

In this experiment, the panel was subjected to airgun impact damage at three locations on the skin side of the panel to assess the criticality of damage location on the residual strength and failure mode. A 0.5-in.-diameter aluminum ball was used to impact the specimen with a velocity of 175 ft/sec at the skin-stiffener flange interface location and 150 ft/sec at two skin locations. One skin location was in the mid-bay of the panel approximately 8 inches below the top potted end and the other location was in the side bay approximately 8 inches above the bottom potted end. The locations of the impact damage are shown in Figure 10. The skin impact in the mid-bay is considered more critical due to the skin local buckling in this region that precedes failure. As the specimen was loaded, failure initiated at the skin-stiffener flange interface location before skin buckling could occur and damage propagated catastrophically across the width of the panel. The failure surface is shown on the right of the figure. The failure load was 118,477 lb which is 13 percent lower than the failure load of the undamaged panel.

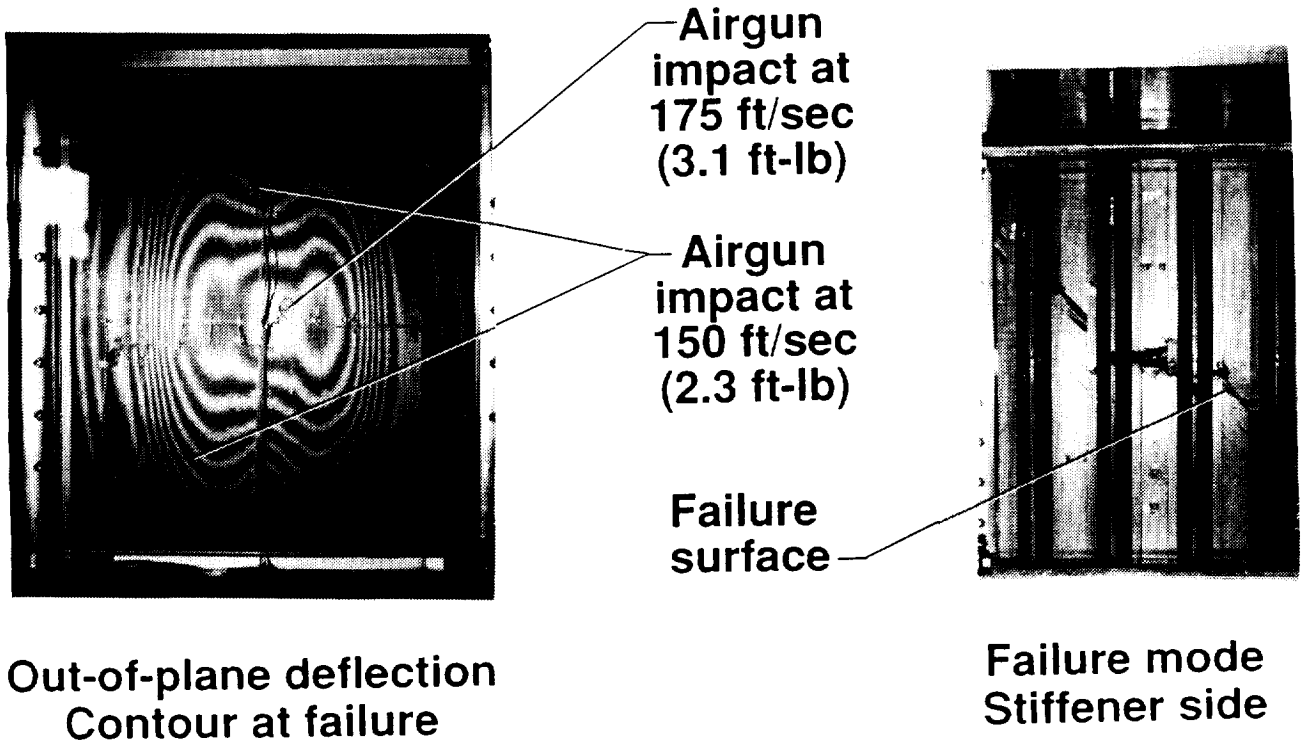

Figure 10. Failure mode of panel specimen subjected to airgun impact.

FAILURE MODE OF PANEL SPECIMEN WITH AIRGUN AND DROPPED-WEIGHT IMPACT DAMAGE

A panel was subjected to a combination of airgun and dropped-weight impact damage and loaded to failure in this experiment. The airgun impact was at 150 ft/sec at the same two skin locations described in the previous test whereas the dropped-weight impact was on the stiffener cap. The stiffener to the left of the center line shown in Figure 11 was impacted at a 15 ft-lb energy level first and then the specimen was loaded to 2/3 of the undamaged failure load for the panel. The panel specimen was then unloaded and the stiffener to the right of the center line of the panel was impacted at a 20 ft-lb energy level before reloading it to failure. When loaded, failure initiated at the skin impact location in the mid-bay and propagated across the width of the specimen. The failure load was 118,887 lb. Considering that the element specimen subjected to a 20 ft-lb dropped-weight impact energy had no degradation in behavior, it appears that damage to the skin is the more critical damage for this foam-filled stiffener concept.

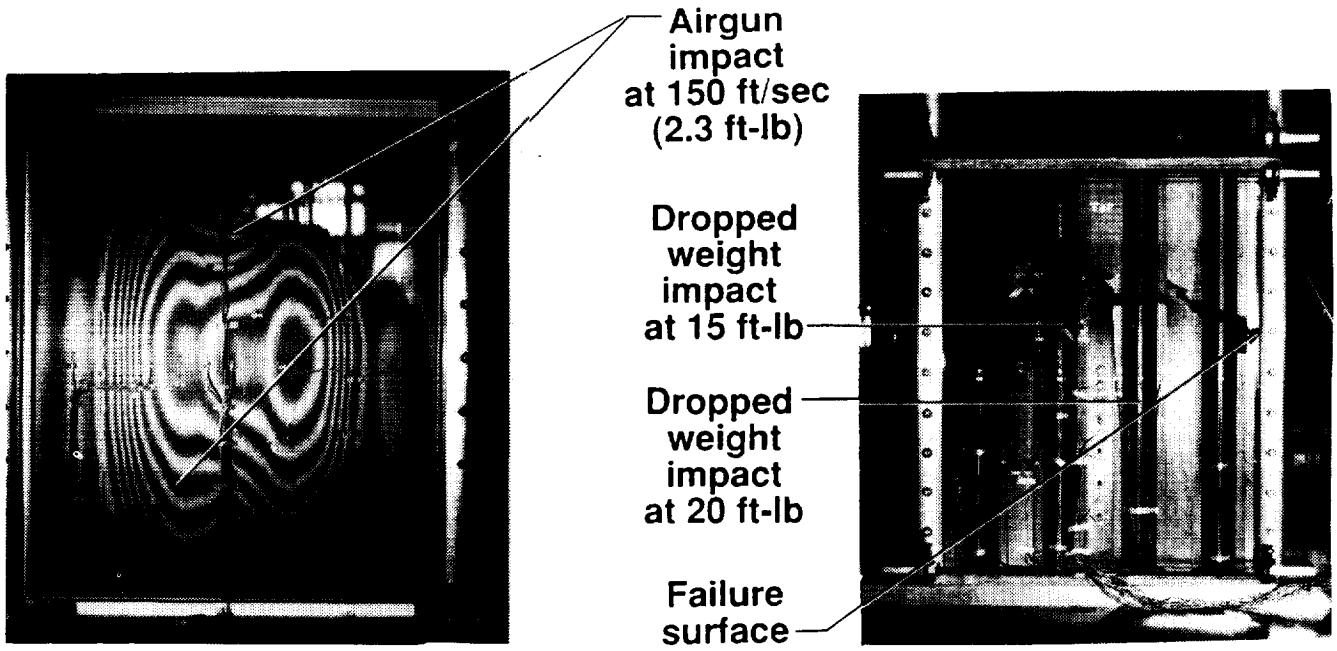

Figure 11. Failure mode of panel specimen subjected to airgun and dropped-weight impact.

END-SHORTENING RESPONSE FOR PANEL TEST SPECIMENS

The panel specimen end-shortening results are summarized in Figure 12. The out-of-plane displacement results normalized by the length of the specimen are plotted as a function of the total applied load normalized by the axial stiffness. The responses of all the panel specimens tested are nonlinear. Compared to the undamaged panel results, both damaged panels exhibit degradation of 13 percent in load carrying ability. The response of the panel subjected to a 15 ft-lb dropped-weight impact falls on top of the response of the panel with a 20 ft-lb impact suggesting that damage due to the 15 ft-lb impact did not result in a stiffness degradation. For all the three panel specimens tested to failure, the global strain at failure is approximately 5,500μ in./in.

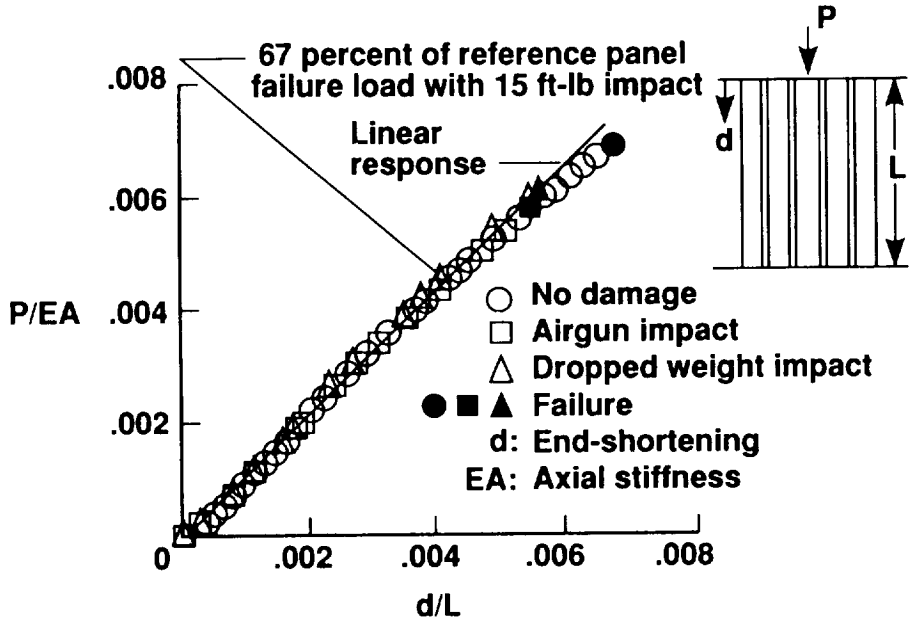

Figure 12. Summary of load versus end-shortening results for panel test specimens.

TYPICAL STRAIN RESULTS FOR PANEL TEST SPECIMENS

The strain results in the skin at mid-length for the panel test specimens are presented in Figure 13. The specimens behaved well and exhibited consistent response in all cases. In the case of the undamaged panel, the skin buckles at approximately 125,000 lb as indicated by the strain reversal in one of the back-to-back gages. The out-of-plane displacement contours obtained from moire interferometry confirmed local skin buckling in the mid-bay of the panel at this load value. The strain levels in the skin of the damaged specimens corresponding to the failure event are approximately 7,000μ in./in.

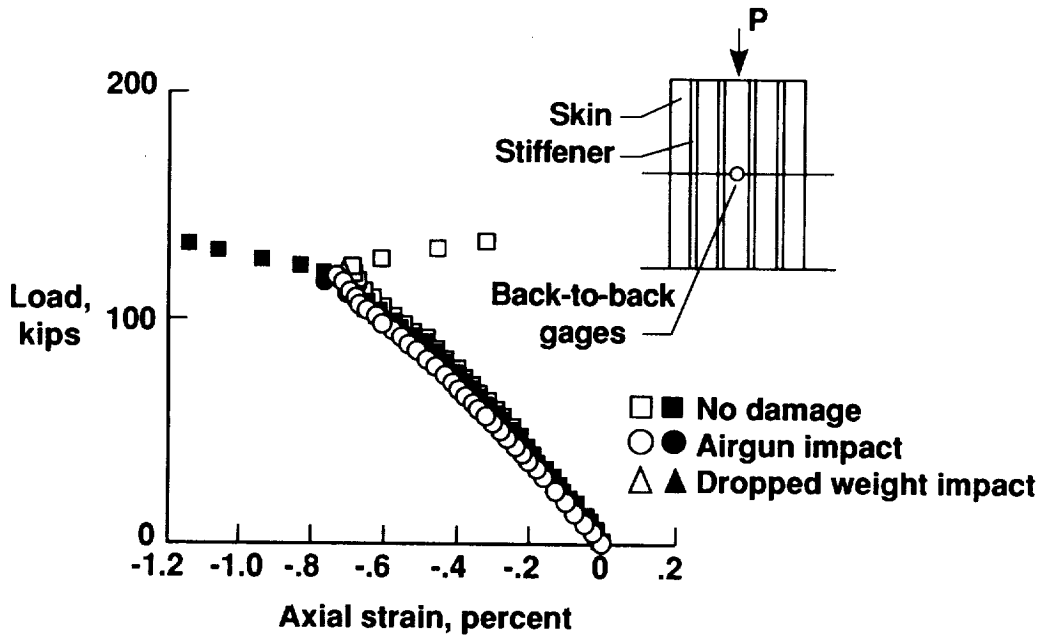

Figure 13. Strain results for panel test specimens at a skin location.

CORRELATION OF ANALYTICAL AND EXPERIMENTAL RESULTS FOR ELEMENT SPECIMEN

The experimental end-shortening results for the element specimen are compared with analytical results in Figure 14. Although linear static and bifurcation buckling analyses for the specimen were performed prior to testing to make instrumentation and loading decisions, geometrically nonlinear static analysis was performed after the test to correlate the displacement and strain results. The DIAL finite element code (Ref. 4) was used to perform buckling and nonlinear static analyses. The analysis results obtained by using the modified Newton-Raphson method are presented as a solid line in the figure. The experimental results are presented as open circles with the failure event indicated by a filled circle. The correlation between the results is good.

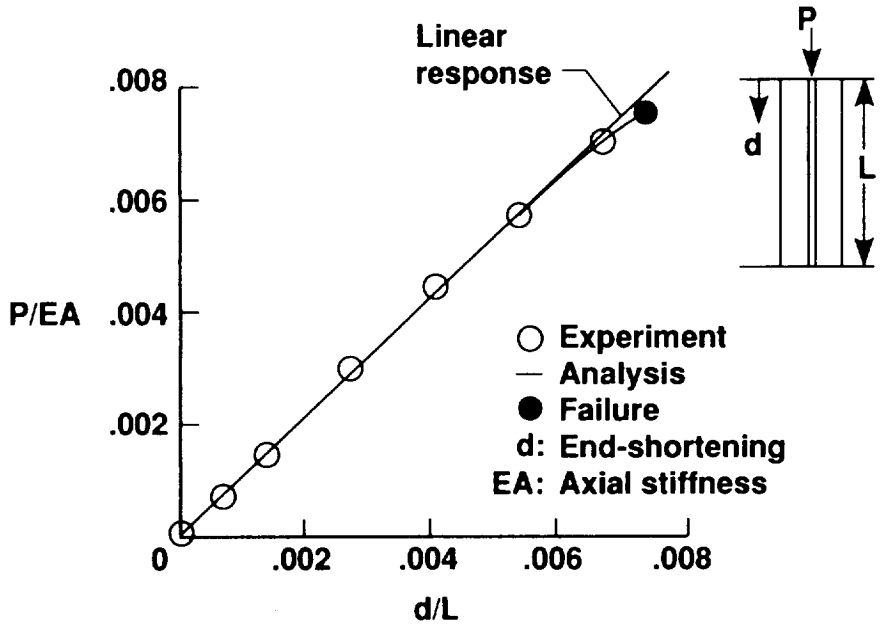

Figure 14. Correlation of element specimen end-shortening results.

CORRELATION OF ELEMENT TEST SPECIMEN BUCKLING RESPONSE

Experimental buckling response of the element test specimen is compared with the finite element analysis result in Figure 15. From moire interferometry and strain results it appears that the element specimen skin buckled into a six half-wave pattern at approximately 33,625 lb. The analysis predicts this first buckling mode at 34,502 lb with the same number of half-waves.

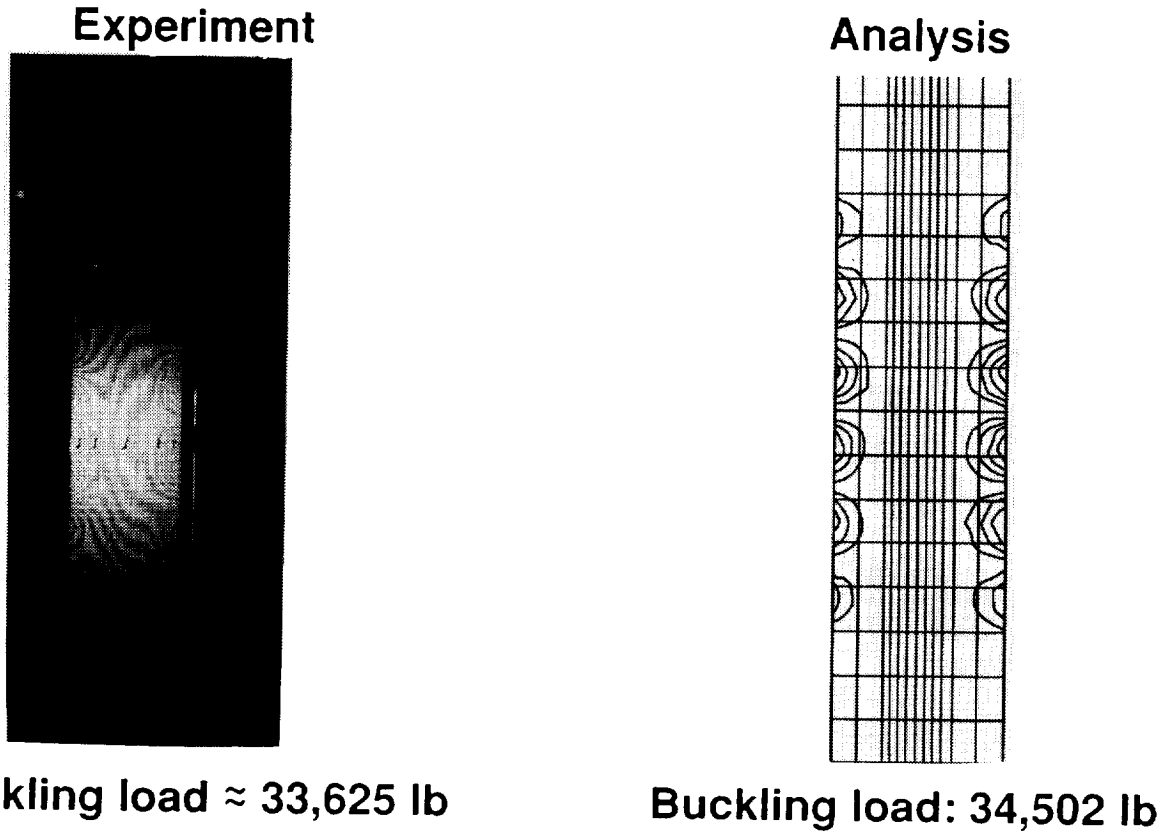

Figure 15. Element test specimen buckling response.

CORRELATION OF ANALYTICAL AND EXPERIMENTAL RESULTS FOR PANEL SPECIMEN

Nonlinear analysis of the panel specimen was performed using the DIAL finite element code and the end-shortening results are compared with experimental results in Figure 16. The finite element model was generated using shear deformable plate elements resulting in a 16,500 degree-of-freedom model when appropriate boundary conditions were imposed. The analytical results are represented in the figure by a solid line and the experimental results are represented by open squares with the filled square representing the failure event. The specimen nonlinear response compares well with the analytical results.

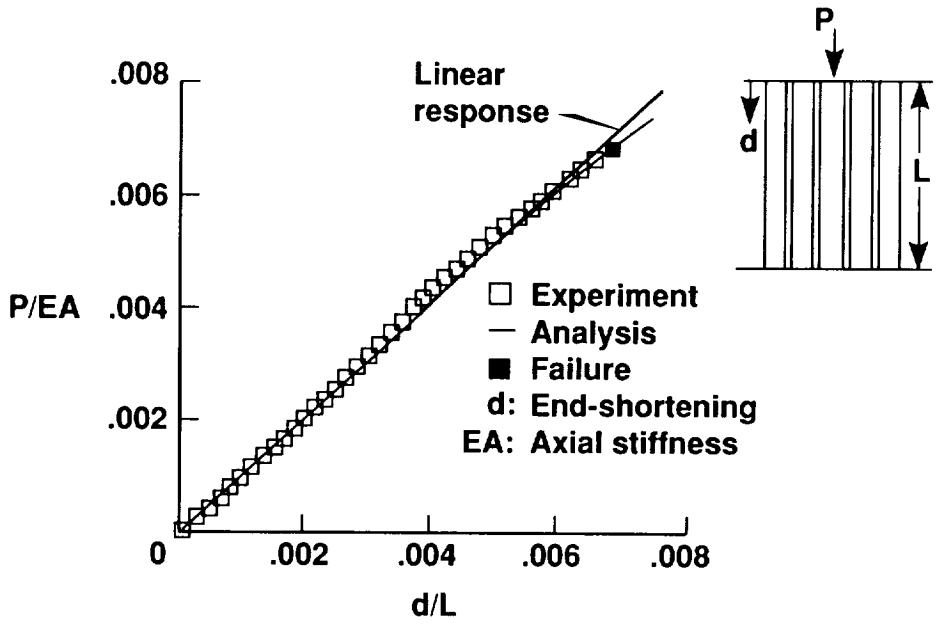

Figure 16. Correlation of panel specimen end-shortening results.

COMPARISON OF PANEL SPECIMEN STATIC RESPONSE AT 75,000 LB

The analytical results for panel static response are compared with the experimental results in Figure 17. As described earlier, the panel exhibited observable out-of-plane displacement beyond 50,000 lb in the form of two lobes at the central stiffener locations. The nonlinear analysis results are compared with the experimental results at 75,000 lb in the figure. The comparison between the analytical and experimental out-of-plane displacement shape and location is good.

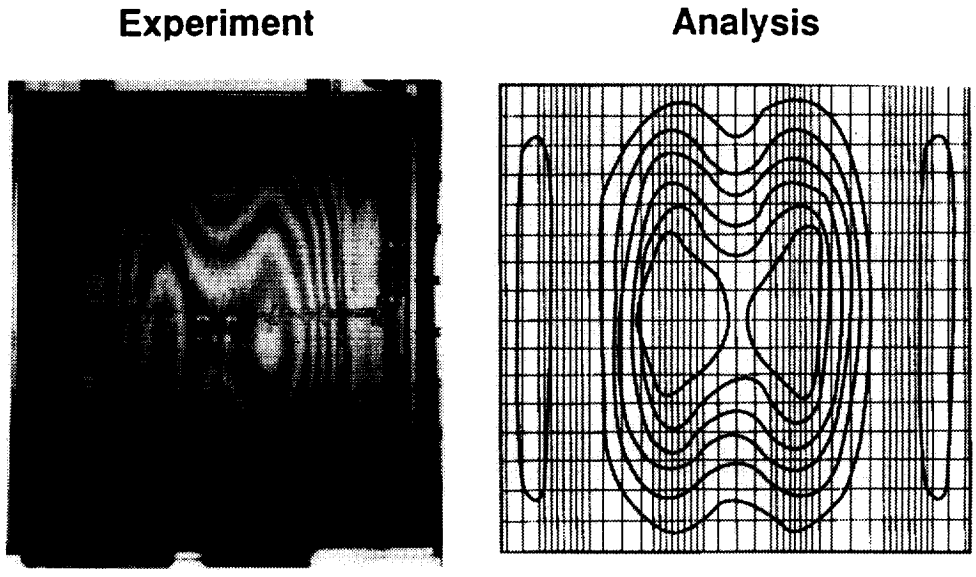

Figure 17. Out-of-plane displacement results for panel specimen at 75,000 lb.

CONCLUDING REMARKS

Design, analysis, and experimental studies have been conducted to evaluate a foam-filled hat-stiffened panel concept. Design studies suggest that using this new concept could result in 6 to 10 percent improvement in structural efficiency compared to the more conventional hat-stiffened panel. The foam-filled hat-stiffened concept is amenable to automated manufacturing processes that are suitable for solid-blade-stiffener geodesic structures and are 20 percent lighter than the solid-blade-stiffener panels in the 3,000 to 20,000 lb/in. load range.

Element specimen results indicate that a 20 ft-lb dropped-weight impact damage to the stiffener cap does not result in significant degradation of performance. Panel test results suggest that airgun impact damage to skin or skin-stiffener flange interface results in the most reduction in residual strength. This reduction in load carrying ability is estimated to be 13 percent which is not very significant. From the tests conducted it appears that the foam-filled hat structural concept is tolerant to the type of damage considered. For all test specimens with and without damage, the global failure strain was above 5,500μ in./in. The analysis results for buckling and nonlinear response compared well with the experimental results.

REFERENCES

1. Reddy, A. D.; Rehfield, L. W.; Haag, R. S.; and Wideman, C. B.: Compressive Buckling Behavior of Graphite/Epoxy Isogrid Wide Columns with Progressive Damage. Compression Testing of Homogeneous Materials and Composites, ASTM STP 808, edited by R. Chair and R. Paperino, 1983, pp. 187-199.

2. Ambur, D. R.; and Rehfield, L. W.: Effect of Stiffness Characteristics on the Response of Composite Grid-stiffened Structures. AIAA Paper No. 91-1087, Proceedings of the 32nd Structures, Structural Dynamics, and Materials Conference, April 8-10, 1991, Part 2, pp. 1349-1356.

3. Stroud, W. J.; and Anderson, M. S.: PASCO: Structural Panel Analysis and Sizing Code, Capability and Analytical Foundations, NASA TM-80181, November 1981.

4. Anon.: DIAL Finite Element Analysis System - Version L3D2. Lockheed Missiles and Space Company, July 1987.